Applied Catalysis B: Environmental 129 (2013) 342–350

Contents lists available at SciVerse ScienceDirect

Applied Catalysis B: Environmental

journal homepage: www.elsevier.com/locate/apcatb

Sulfonic acid functionalized mesoporous SBA-15 catalysts for biodiesel production

Donghua Zuo [1], James Lane *, Dan Culy, Michael Schultz, Allison Pullar, Michael Waxman

Department of Natural Sciences and Lake Superior Research Institute, University of Wisconsin-Superior, Superior, WI 54880, United States

ARTICLE INFO

Article history:
Received 30 May 2012
Received in revised form
14 September 2012
Accepted 19 September 2012
Available online 27 September 2012

Keywords:
Mesoporous SBA-15 catalysts
Organosulfonic acid functionalization
Biodiesel
Transesterification
Esterification

ABSTRACT

Sulfonic acid functionalized mesoporous SBA-15 catalysts have been studied in the microwave-assisted transesterification of soybean oil with 1-butanol in order to produce low freezing point biodiesel. Small-angle powder XRD and nitrogen adsorption analysis revealed the formation of mesoporous materials with high surface area and uniform porosity. Catalytic activity was found to be largely dependent on the acid strength rather than the number of acid sites. Propyl-SO_3H and arene-SO_3H functionalized SBA-15 catalysts showed high activity and stability in transesterification reactions whereas perfluoro-SO_3H functionalized SBA-15 catalyst exhibited a complete loss of activity after recycling due to complete leaching of perfluoro-SO_3H groups in the reaction medium. The results over arene-SO_3H functionalized catalysts showed that the optimal loading of arene-SO_3H groups is approximately 15% (molar percent of functional group to total silicon) and the optimal oil to alcohol molar ratio is 1:6. Increases in catalyst to oil weight ratio and reaction temperature significantly enhance the reaction rates. Simultaneous transesterification and esterification of soybean oil with up to 20 wt% oleic acid over arene-SO_3H functionalized catalyst indicated that this catalyst could be a promising candidate for processing low quality feedstocks containing high fraction of free fatty acids. Further modification of Ar-SO_3H SBA-15 catalyst with hydrophobic groups did not significantly improve its catalytic performance.

1. Introduction

Biodiesel, a term describing a mixture of the mono-alkyl esters of vegetable oils or animal fats, is an alternative to conventional diesel fuel. It is renewable, biodegradable, produces less air pollutants than petroleum-based diesel and reduces our dependence on fossil fuels [1,2]. The most commonly used biodiesel production method is transesterification in which the triglyceride molecules present in vegetable oils or animal fats chemically react with short-chain alcohols (e.g. methanol or ethanol) in the presence of a catalyst. The properties of biodiesels vary somewhat depending on the oil feedstocks and alcohols used affecting their use as a substitute for conventional diesel fuel [3,4]. In spite of its desirable properties as a diesel fuel substitute, the production of biodiesel from food-grade oils is currently not economically competitive with conventional diesel fuel due to high raw material and production costs [5]. Waste oils and greases, which are significantly less expensive than food-grade oils, offer an attractive alternative [6–8].

The transesterification reaction is normally catalyzed by an alkaline catalyst such as sodium hydroxide or sodium methoxide. However, several drawbacks related to the homogeneous nature of the catalyst including acid neutralization, water washes and separations have been reported [9]. Furthermore, the recycled waste oils and greases as well as many other low-cost feedstocks usually contain from 10% to 25% free fatty acids (FFA) as well as a certain amount of water [10]. During the transesterification catalyzed by an alkaline catalyst, existing FFAs already present or generated from the hydrolysis of oils and fats with water will react with the catalyst to form soap which reduces reaction rates and product yields and greatly complicates purification in order to meet ASTM biodiesel standards. Extra pretreatment steps to deal with FFAs and water would increase processing costs [5,11].

The use of heterogeneous acid catalysts could be an attractive solution to overcome these disadvantages. As a matter of fact, the use of heterogeneous acid catalysts in the production of biodiesel could vastly simplify catalyst removal, reduce catalyst cost, minimize the amount of waste formed and provide the possibility to process low quality feedstocks with high FFA content since acid catalysts can simultaneously catalyze esterification of FFAs and transesterification of triglycerides [12,13]. Solid acid catalysts

* Corresponding author. Tel.: +1 715 394 8204.
E-mail addresses: zuodonghua@yahoo.com (D. Zuo), jlane@uwsuper.edu (J. Lane).
[1] Present address: DuPont Experimental Station, 200 Powder Mill Road, Wilmington, DE 19803, United States.

0926-3373/$ – see front matter © 2012 Elsevier B.V. All rights reserved.
http://dx.doi.org/10.1016/j.apcatb.2012.09.029

used in esterification and transesterification reactions include acid resins [14–16], supported heteropolyacids [17–19], or sulfated or tungstated zirconia [16,20–24]. At low temperatures, the activity of solid acid catalysts in transesterification is normally quite low, and to obtain a sufficient reaction rate, it is necessary to increase the reaction temperature (>170 °C). The sulfonic acid resins such as Amberlyst-15 cannot be used because they are not stable at these temperatures [9]. Heteropolyacid and sulfated or tungstated zirconia catalysts, being inorganic oxides, can be used at higher temperatures. However, the activity of these catalysts is still relatively low because of their relatively weak acidity, small surface area and pore size. In this regard, sulfonic acid functionalized mesoporous SBA-15 materials could be an interesting alternative since the open mesoporous structure, high surface area and large pore size could provide a sufficient number of catalytically active sites and minimize the diffusion limitations for large molecules with long alkyl chains in porous solids [25–27].

While mesoporous solid acid catalysts could vastly simplify the biodiesel production, higher temperatures are needed to reach comparable reaction rates than in the case of the homogeneous alkaline catalysts (60–80 °C). Higher temperatures necessarily mean more energy input is required to heat the reaction mixture. A microwave-assisted reactor provides an attractive option for carrying out the transesterification and esterification reactions at higher temperatures. Compared with conventional thermal heating, microwave irradiation can transfer energy directly into the reactants, thus offering a fast, easy route with advantages of a short heating time for the reaction mixture to reach the desired temperature, a short reaction time, a low alcohol/oil ratio and ease of operation [28–30].

In the present work, mesostructured SBA-15 catalysts functionalized by different sulfonic acid groups (propyl-SO_3H, arene-SO_3H, perfluoro-SO_3H) have been synthesized and studied in the microwave-assisted transesterification of soybean oil with 1-butanol. Transesterification of soybean oil using 1-butanol as alcohol source, in part, was to address the poor low temperature flow property issue associated with conventional methyl or ethyl ester type biodiesel. These conventional biodiesels have considerably higher crystallization temperature than diesel fuel. The use of branched esters such as iso-propyl, iso-butyl and 2-butyl instead of the methyl esters can effectively improve the low temperature properties [31–33]. In addition, an advantage of 1-butanol in comparison with methanol is its higher boiling point. This indicates that transesterification reactions can be conducted at higher temperatures without reaching extremely high autogenic pressures when the reactions are performed in a closed vessel [30]. Subsequently, the influences of functional group loading and several operation variables as well as performance in simultaneous esterification and transesterification reactions have been investigated over the arene-sulfonic acid functionalized catalyst – one of the mesostructured acid catalysts showing good catalytic performance. Surface modification of the arene-sulfonic acid functionalized catalyst by hydrophobic groups has also been assessed. These results as well as characterization of the catalysts will be discussed.

2. Experimental

2.1. Materials

Soybean oil (Aldrich) and 1-butanol (Aldrich) were used as feedstocks for transesterification reactions. Tetraethyl orthosilicate (TEOS, 98%, Aldrich) was used as silica precursor in the synthesis of silica-based mesostructured materials. (3-Mercaptopropyl) trimethoxy silane (MPTMS, 95%, Aldrich), 2-(4-chlorosulfonyl phenyl) ethyltrimethoxy silane (CSPTMS, ACROS) and 1,2,2-trifluoro-2-hydroxy-1-trifluoromethylethanesulfonic acid sultone (Matrix Scientific) were used as precursors for incorporation of different sulfonic acid groups. Pluronic (P123, Aldrich) was used as a template in the synthesis of mesostructured materials. Commercially available Amberlyst-15 (Rohm Haas) was used as a reference catalyst.

2.2. Synthesis of sulfonic acid functionalized mesoporous SBA-15 materials

2.2.1. Propyl-SO_3H SBA-15 (Pr-SO_3H)

Propyl-sulfonic acid functionalized SBA-15 material was synthesized by following the one-step co-condensation procedure described in the literature [25,26,34–36]. 4 g of P123 was dissolved in 125 g of 1.9 M HCl at room temperature under stirring. The clear solution was subsequently heated to 40 °C before adding TEOS. The resultant white suspension was stirred for 1 h for TEOS prehydrolysis before the addition of MPTMS together with H_2O_2 (30 wt%) used as oxidant. The resultant mixture, with a molar composition of 0.0369 TEOS:0.0041 MPTMS:0.0369 H_2O_2:0.24 HCl:6.67 H_2O, was stirred at 40 °C for 20 h and thereafter aged at 100 °C for an additional 24 h under static conditions. The solid material was recovered by filtration and washed with ethanol under reflux for 24 h to extract the template. The final material was oven-dried at 100 °C overnight.

2.2.2. Arene-SO_3H SBA-15 (Ar-SO_3H)

Arene-sulfonic acid functionalized SBA-15 materials were also synthesized by following the one-step co-condensation procedure described in the literature [25,26,35,36]. Following the above described TEOS prehydrolysis, CSPTMS (50 wt% in dichloromethane) was added and the resultant mixture was stirred at 40 °C for 20 h and thereafter aged at 100 °C for an additional 24 h under static conditions. The solid material was recovered and extracted as previously described. The molar composition of the different mixtures for 4 g of copolymer P123 was $0.041(1-X)$ TEOS:$0.041X$ CSPTMS:0.24 HCl:6.67 H_2O, where X is the molar fraction of TEOS replaced by CSPTMS. The loadings of Ar-SO_3H functional groups (molar fraction of functional groups to total silicon, i.e. CSPTMS/(CSPTMS + TEOS)) ranged from 5% to 20%. The resultant catalyst materials were denoted as Ar-SO_3H-X.

2.2.3. F-SO_3H SBA-15 (F-SO_3H)

This material was synthesized through a post-synthetic method, following the procedure reported by Melero et al. [26]. Typically, 2 g of calcined pure SBA-15 material was suspended with 1 g of perfluorosulfonic acid precursor in 50 mL of dry toluene under reflux for 16 h under nitrogen atmosphere before recovering the material by filtration. The resultant material was thoroughly washed with fresh toluene and oven-dried at 100 °C overnight.

2.2.4. Modified arene-SO_3H SBA-15

The Ar-SO_3H-10 catalyst was modified by capping with methoxytrimethyl silane using a post-synthetic procedure [26] and methylation with methyltriethoxy silane using a one-step synthetic procedure [27,34]. In the one-step synthesis, the procedure was the same as the preparation of Ar-SO_3H-10 except that 0.38 g of methyltriethoxy silane was added at the same time as CSPTMS. The molar composition of the resultant mixture for 4 g of copolymer was 0.0349 TEOS:0.0041 CSPTMS:0.0021 methyltriethoxy silane:0.24 HCl:6.67 H_2O. The catalytic material was denoted as M-Ar-SO_3H-10. For the post-synthetic grafting procedure, 1 g of pre-dried Ar-SO_3H-10 material was suspended with 1 g of trimethylmethoxy silane in 70 mL of dry toluene under reflux for 16 h before recovering the material by filtration. The final

materials prepared in two different ways were oven-dried at 100 °C overnight.

2.3. Catalyst characterization

The textural properties of the catalysts were analyzed through N_2 adsorption–desorption isotherms in a Micromeritics ASAP-2020 instrument. Structural ordering was measured by means of small angle X-ray powder diffraction on a Panalytical X'pert PRO MFD X-ray diffractometer using CuKα radiation in the 2θ angle range of 0.4–2° with a 0.01° step size and a collection time of 8 s per step. The amount of incorporated sulfonic groups was calculated through the sulfur content determined by a CM5014 sulfur Coulometer. Acid capacities of the functionalized mesoporous materials were determined using aqueous solutions of sodium chloride (NaCl, 2 M) and tetramethyl ammonium chloride (TMACl, 0.05 M) as exchange agents and 0.01 M NaOH aqueous standard solution as titration agent [34].

2.4. Catalytic tests

All catalysts were tested in a CEM 600155 microwave reactor system. In a typical run, 3.0 g of soybean oil, 1.53 g of 1-butanol and 150 mg of catalyst (5 wt% referred to the amount of oil) were placed together inside a 10 mL glass reaction vial which was placed within the reactor system. Next the reaction vial was heated and maintained at the set temperature using a microwave power of 300 W while stirring with a magnetic stir bar at high speed. The time required to reach the set temperature was approximately 1 min. The reactions were performed at the set temperature for up to 30 min. The reaction vial was cooled down rapidly to 50 °C for sampling every 5 min using cooling air, and 10 μL of the homogeneous (thoroughly mixed) reaction mixture was collected for analysis. Reaction samples were diluted with *n*-heptane to 1.5 mL and analyzed by an Agilent 1200 series HPLC equipped with an evaporative light scattering detector (ELSD), from which triglycerides, diglycerides, monoglycerides and butyl esters were separated and quantified. The yield of biodiesel was calculated by dividing the amount of butyl esters by the sum of unconverted glycerides and butyl esters in the sample. Three blank tests by following the same procedure without adding any catalyst were performed at 190 °C, 210 °C and 240 °C, respectively, and there was no detectable butyl ester formation, indicating the conversion to biodiesel in the absence of catalyst is negligible.

2.5. Catalyst reusability tests

The catalysts separated from the reaction mixture by centrifugation were double-washed with methanol and *n*-hexane (10 mL solvent each time) to remove both polar and non-polar compounds adsorbed on the catalysts. Then catalysts were dried at 100 °C prior to being reused in the recycling tests.

3. Results and discussion

3.1. Sulfonic acid functionalized SBA-15 catalysts containing various organosulfonic groups

The physicochemical and textural properties of pure SBA-15 and functionalized SBA-15 materials containing three different sulfonic acid groups are summarized in Table 1. The BET surface area, pore size, d_{100} spacing and average pore wall thickness are in the range as reported in the literature for these types of mesoporous materials [25,26,34–36]. The N_2 adsorption–desorption isotherms of the synthesized materials are shown in Fig. 1A. All isotherms display a steep Type IV hysteresis loop in the range of relative pressures of 0.6–0.8, in accordance with the literature results for these types of materials [26,34–36]. Among the three functionalized catalysts, F-SO_3H has the smallest surface area and largest pore size whereas Ar-SO_3H-10 has the smallest pore size. The surface areas of Pr-SO_3H-10 and Ar-SO_3H-10 are comparable to that of pure SBA-15. The small-angle XRD patterns of the synthesized materials are shown in Fig. 1B. A single prominent reflection centered at 2θ below 1° can be assigned to the crystallographic direction [1 0 0], which is the typical signal for hexagonally ordered mesophases. Low-intensity signals can be assigned to directions [1 1 0] and [2 0 0], indicative of long-range hexagonal ordering [34,37]. The XRD peaks for Pr-SO_3H-10 and Ar-SO_3H-10 samples shift slightly to lower angles, resulting in small increases in d_{100} spacing. This feature can be explained by the presence of larger organic moieties compared with the other silica precursor, tetraethyl orthosilicate, in the one-step co-condensation synthetic process. In contrast, an identical XRD peak was measured for the F-SO_3H sample as compared to that for pure SBA-15 sample, which could be explained by the fact that the F-SO_3H sample was prepared by a post-synthetic method following the synthesis of pure SBA-15. It appears that the post-modification process did not change the unit cell parameters (d_{100}) but decreased the surface area of the post-synthesized material, possibly due to pore blocking.

The sulfur content in the sulfonic acid functionalized SBA-15 materials was analyzed by a Sulfur Coulometer, and the number of accessible organosulfonic acid sites was determined by potentiometric titration method after ion exchanged with NaCl and TMACl, respectively. The results are listed in Table 1 and are in agreement with those reported in the literature [26,34] as well. Since the F-SO_3H material is not stable in polar media, its acid capacity was not measured by titration. Consistent results were obtained from the

Table 1
Textural and acid properties of sulfonic acid functionalized SBA-15 materials.

Sample	XRD		Textural properties			Acid properties[e]		
	d_{100}[a] (Å)	Wall thickness[b] (Å)	BET area (m^2/g)	Pore size[c] (Å)	Pore volume[d] (cm^3/g)	Sulfur (mequiv./g)	NaCl exchange (mequiv./g)	TMACl exchange (mequiv./g)
SBA-15	104	54.0	823	66	1.29	–	–	–
Pr-SO_3H-10	113	58.5	772	72	1.44	1.12	1.21	1.08
Ar-SO_3H-10	109	68.9	805	57	1.08	1.07	1.15	1.14
F-SO_3H	105	42.2	522	79	1.15	0.31	–	–

[a] d_{100} spacing measured from small-angle X-ray diffraction.
[b] Average pore wall thickness calculated by a_0-pore size ($a_0 = 2 \times d_{100}/\sqrt{3}$).
[c] Average pore size from adsorption branch applying the BJH model.
[d] Pore volume was taken at $P/P_0 = 0.985$ single point.
[e] Acid capacity defined as milliequivalents of acid centers per gram of catalyst, obtained either directly by titration or indirectly from the sulfur content by elemental analysis.

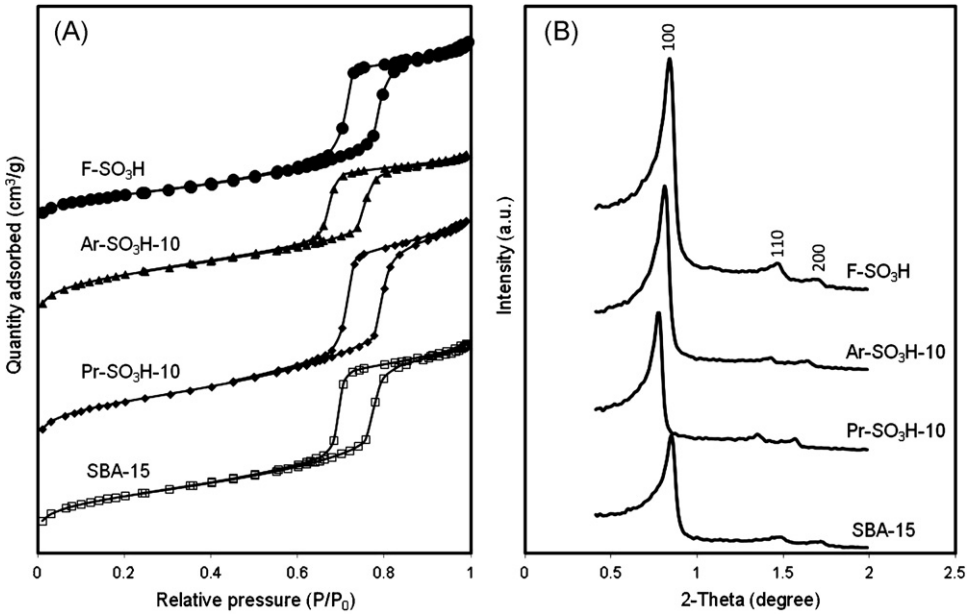

Fig. 1. (A) N_2 adsorption–desorption isotherms at 77 K, and (B) small-angle XRD patterns of sulfonic acid functionalized SBA-15 catalysts.

two different methods. The acid capacities of Pr-SO_3H-10 and Ar-SO_3H-10 catalysts are comparable whereas the F-SO_3H catalyst has a much lower acidity. The difference in acid capacities determined by titration after ion exchanged with NaCl and TMACl, respectively, for Pr-SO_3H-10 catalyst is larger than that for Ar-SO_3H-10 catalyst, possibly indicating more micropores are present on Pr-SO_3H-10 catalyst.Fig. 2 presents the catalytic activity of three sulfonic acid functionalized SBA-15 catalysts in the transesterification of soybean oil with 1-butanol. Among them, the F-SO_3H catalyst is the most active catalyst, exceeding the commercial Amberlyst-15 catalyst. The acid measurements indicated that F-SO_3H catalyst has a much lower acid capacity compared with the other two catalysts while the acid capacities for Pr-SO_3H-10 and Ar-SO_3H-10 catalysts are comparable (Table 1). This observation would suggest that the activity order of the organosulfonic acid functionalized mesoporous catalysts largely depends on the acid strength instead of the number of acid sites. The different nature of the molecular environment of the SO_3H sites in these three similar catalysts defines their acid strength. More electron withdrawing environments provide higher acid strength, leading to higher catalytic activity in transesterification reactions. Melero et al. [27] presented ^{31}P NMR signal shifts of chemisorbed trimethylphosphine oxide over arenesulfonic SBA-15 material toward high values in comparison to that obtained for alkylsulfonic SBA-15 material, confirming enhancement of the acid strength due to the presence of a more electron-withdrawing substituents. Miao and Shanks [36] also reported that the activity of arenesulfonic-modified SBA-15 in the esterification of fatty acids with methanol was significantly higher than that shown by propylsulfonic acid functionalized SBA-15.

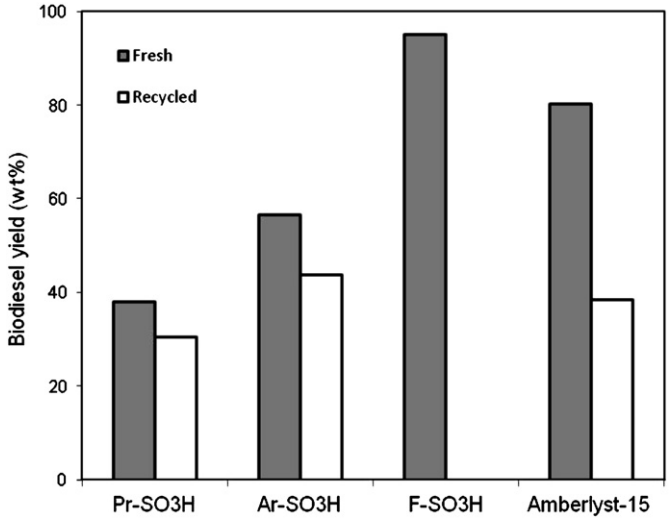

Fig. 2. Catalytic activity and reusability of sulfonic acid functionalized SBA-15 catalysts in the transesterification of soybean oil with 1-butanol compared with Amberlyst-15. Reaction conditions: 3.0 g of soybean oil, 1.53 g of 1-butanol, 150 mg of catalyst, 190 °C, 15 min.

3.2. Catalyst reusability

After recycling by solvent washing, the activity level of the Pr-SO_3H-10 and Ar-SO_3H-10 catalysts was about 85–90% of the fresh catalyst activity. The activity loss could be mainly due to some loss of catalyst materials during the recycling and washing steps. Less than 50% of the activity for Amberlyst-15 remained because this sulfonic acid resin is not thermally stable at 190 °C [9]. However, the F-SO_3H catalyst completely lost its activity after recycling by solvent washing due to the incorporated functional groups being completely leached from the SBA-15 substrate in the reaction medium. This result has been confirmed in two separate reaction runs: one by removing the catalyst solids from the reaction mixture after 5 min and continuing the reaction in the liquid mixture for 25 min and the other by mixing new feedstocks with the separated catalyst solids and running the reaction for 30 min. The biodiesel yields obtained from the former experiment were almost the same as in the case of running the reaction for 30 min without catalyst separation whereas in the latter experiment, the separated catalyst after reaction at 190 °C for 5 min did not show any activity by mixing with fresh samples of the feedstock.

In order to confirm the ease of function group leaching from the F-SO_3H catalyst in polar media, 250 mg of said catalyst was soaked in 2.55 g of 1-butanol for 1 h at room temperature. After recovering by filtration, washing with methanol twice and oven-drying at 100 °C, the obtained material was analyzed by Sulfur Coulometer.

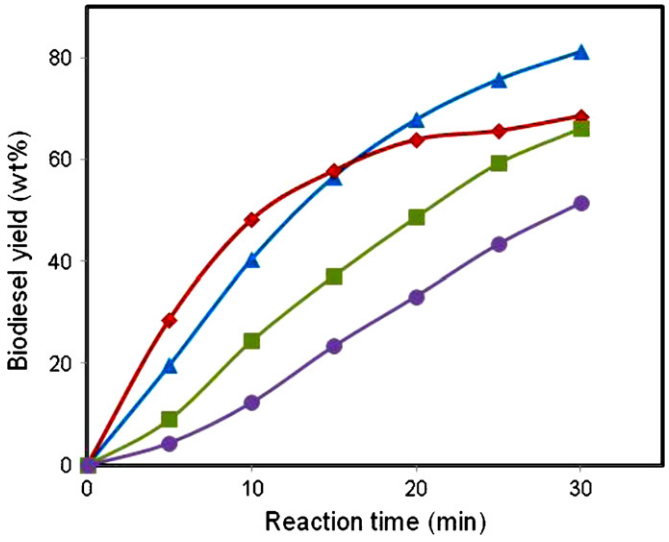

Fig. 3. Effect of 1-butanol to oil molar ratio on biodiesel yield over Ar-SO_3H-10 catalyst. Reaction conditions: 3 g of soybean oil, 150 mg of catalyst, 190 °C, 30 min, alcohol to oil molar ratio (♦) 3:1, (▲) 6:1, (■) 9:1, (●) 12:1.

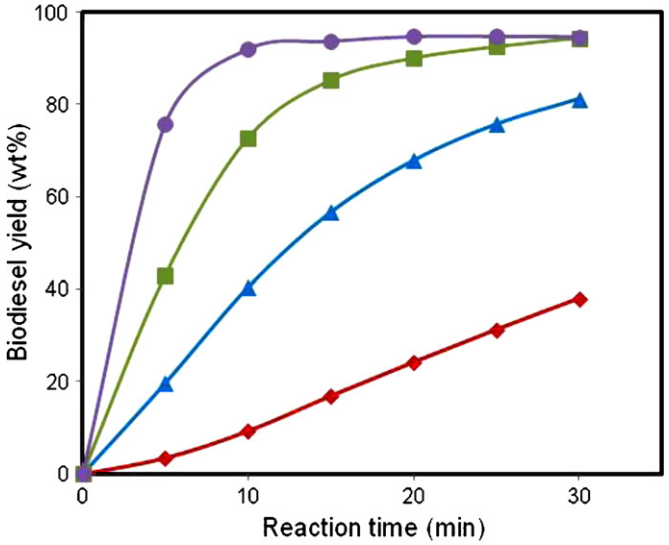

Fig. 4. Effect of catalyst weight on biodiesel yield over Ar-SO_3H-10 catalyst. Reaction conditions: 3 g of soybean oil, 1.53 g of 1-butanol, 190 °C, 30 min, catalyst to oil weight percent (♦) 2%, (▲) 5%, (■) 10%, (●) 15%.

Only a trace amount of sulfur was measured. The instability of F-SO_3H group in the functionalized SBA-15 catalyst synthesized by following the same procedure was reported by Melero et al. [26]. The experimental results indicated that Si—O—C bonding in the perfluorosulfonic acid functionalized catalyst is not stable under the reaction conditions as compared to the Si—C bond present in the Pr-SO_3H and Ar-SO_3H catalysts.

3.3. *Effect of alcohol to oil ratio, catalyst weight and reaction temperature over Ar-SO_3H-10 catalyst*

After identifying the Ar-SO_3H functionalized SBA-15 material as a good catalyst on the basis of initial screening under the reaction conditions, the effect of several operation variables was investigated.

Fig. 3 shows the influence of alcohol to oil molar ratio on biodiesel yield over Ar-SO_3H-10 catalyst. The alcohol to oil molar ratio was varied from 3:1 to 12:1. It is apparent that the initial reaction rate is largely dependent on the concentration of oil in the reaction mixture. By comparison, the 3:1 alcohol to oil molar ratio gave rise to the fastest initial reaction rate but seemingly led to a lower equilibrium biodiesel yield. Further increasing the alcohol to oil ratio led to decrease in oil concentration and accordingly decrease in reaction rate. Under the present reaction conditions, the optimal alcohol to oil molar ratio is 6:1.

Fig. 4 depicts the influence of the amount of the catalyst charged into the reactor on the biodiesel yield over Ar-SO_3H-10 catalyst. The catalyst amount was varied from 2% to 15% (weight percent of catalyst to soybean oil) at a temperature of 190 °C and alcohol to oil molar ratio of 6:1. As the amount of the catalyst increased, the rate at which reaction equilibrium was reached also increased due to the increase in the total number of active sites available for the reaction. In a typical run (5 wt% of catalyst to oil), the reaction did not reach the equilibrium within 30 min of reaction time. As the catalyst amount was increased to 10 wt%, equilibrium was reached at 30 min with 95% biodiesel yield. When 15 wt% of catalyst was charged, the equilibrium was reached within 10 min. The increase in catalyst concentration considerably shortened the time needed to reach the reaction equilibrium but did not change the biodiesel yield at equilibrium.

It is worthwhile to note that the initial reaction rate (the biodiesel yield at the reaction time of 5 min) increased more than proportionally to the increase in catalyst amount. For example, the biodiesel yield was 20 wt% at 5 min using 5 wt% catalyst while the biodiesel yield was 76 wt% at 5 min using 15 wt% catalyst. A 3-fold increase in catalyst amount led to an almost 4-fold increase in reaction rate. In general, an increase in catalyst amount will increase the number of active sites available for the adsorption of the reactants resulting in a more rapid increase in the number of sites of interaction between the reactants. This observation might be due to a cooperation effect between the increased active sites or could be interpreted as the reaction being of higher order (>1) with respect to the catalyst concentration.

In order to investigate the catalyst thermal stability at higher temperatures, the reaction temperature was increased from 190 °C to 210 °C and 240 °C. The results are shown in Fig. 5. The reaction temperature in this range has a direct influence on the reaction rate. At 210 °C, the initial reaction rate almost doubled compared to that at 190 °C. Equilibrium with 90 wt% biodiesel yield was reached at 20 min of reaction time using 5 wt% of catalyst. When the reaction

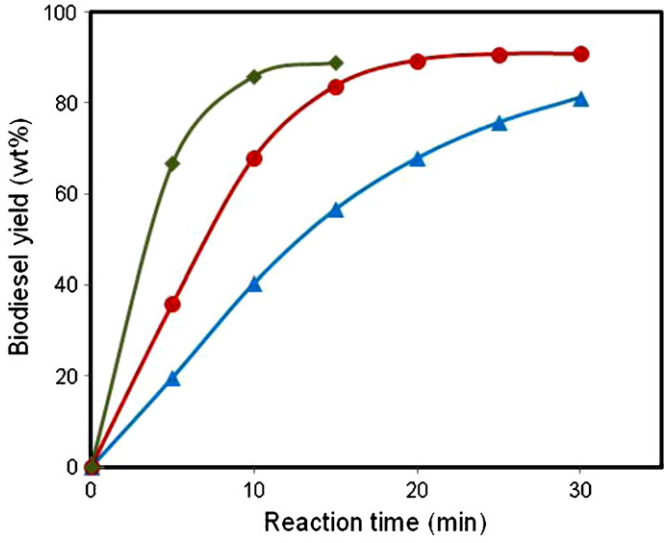

Fig. 5. Effect of reaction temperature on biodiesel yield over Ar-SO_3H-10 catalyst. Reaction conditions: 3 g of soybean oil, 1.53 g of 1-butanol, 150 mg of catalyst, 30 min, reaction temperature (▲) 190 °C, (●) 210 °C, (♦) 240 °C.

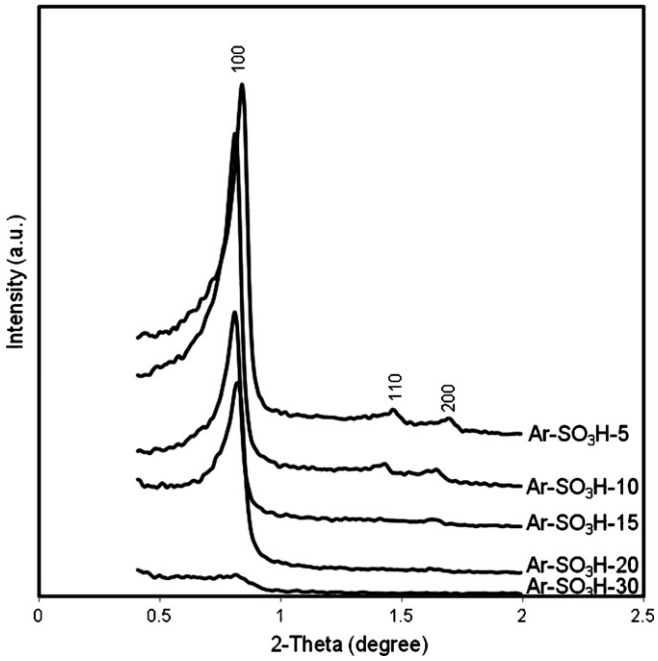

Fig. 6. Small-angle powder XRD patterns for Ar-SO_3H modified SBA-15 catalysts with variable functional group loadings (5%, 10%, 15%, 20%, 30%).

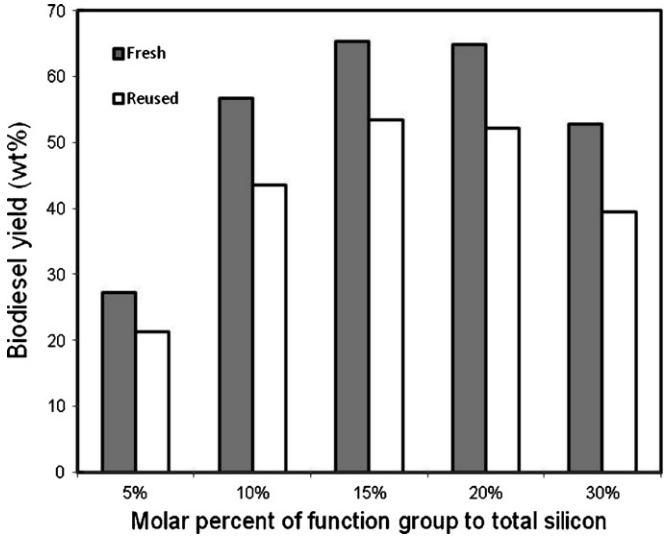

Fig. 7. Catalytic activity and reusability of Ar-SO_3H modified SBA-15 catalysts with variable functional group loadings. Reaction conditions: 3.0 g of soybean oil, 1.53 g of 1-butanol, 150 mg of catalyst, 190 °C, 15 min.

temperature was further increased to 240 °C, the initial reaction rate doubled again and the equilibrium was reached within about 10 min. The catalysts used at 210 °C and 240 °C, respectively, were also recycled by solvent washing and drying. Similar activity recovery of 85–90% was obtained as for the catalyst tested at 190 °C, indicating that this catalyst material is essentially thermally stable under the reaction conditions when the reaction temperature was even as high as 240 °C.

3.4. Ar-SO_3H modified SBA-15 catalysts with variable function group loadings

Ar-SO_3H modified SBA-15 catalysts with variable function group loadings (molar percent of function group to total silicon) were synthesized and their physicochemical and textural properties were summarized in Table 2. It can be seen that the two catalysts with 5% and 10% function group loadings have similar textural properties. When the function group loading was higher than 15%, the surface area and pore volume decreased considerably while the pore size did not change significantly. Fig. 6 shows the small-angle XRD patterns of these catalysts. As the function group loading increases, the XRD patterns show increasing disorder as indicated by the diminishing reflection peaks. The hexagonally ordered mesostructures were measured on all catalysts with function group loadings less than 20% whereas the hexagonal order diffraction peak is nearly gone on the Ar-SO_3H-30 catalyst. Low-intensity signals were observed on Ar-SO_3H-5, Ar-SO_3H-10 and Ar-SO_3H-15 samples indicating long-range hexagonal ordering. Among these five catalysts, Ar-SO_3H-5 has a d_{100} spacing of 105 Å, similar to that in pure SBA-15 sample while the d_{100} spacing for the rest of the catalysts with function group loading higher than 10% slightly increased. It appears that the very small function group loading (5%) during the co-condensation did not change the prehydrolyzed SBA-15 structures whereas the presence of a high concentration (above 10%) of arene-sulfonic acid groups in the co-condensation disturbed the formation and self-assembly of the mesophases [34], resulting in slightly increased *d*-spacings. Meanwhile, the presence of large quantity of arene-sulfonic acid groups during the co-condensation might lead to the collapse of the prehydrolyzed SBA-15 structures which in turn resulted in a drastic decrease in total surface area and the pore volume. The Ar-SO_3H-30 catalyst is essentially an amorphous material.

The acid properties of Ar-SO_3H modified SBA-15 catalysts with variable function group loadings were measured by Sulfur Coulometer and potentiometric titration and listed in Table 2. Consistent acid capacities were also obtained via different techniques. As the function group loading increases, the number of acid sites correspondingly increases. For the catalysts with function group loading above 20%, the number of acid sites accessible to Na^+ is more than that accessible to TMA^+, indicating more micropores are present on the high function group loading catalysts.

The catalytic testing results over Ar-SO_3H modified catalysts with variable function group loadings are shown in Fig. 7. When the functional group loading was initially increased from 5% to 10%, the catalyst activity increased proportionally with the increase in acid capacity as shown in Table 2. A maximum activity was achieved using the catalyst with 15% functional group loading. When the functional group loading was further increased, the catalyst activity decreased even though an increase in acid capacity was measured. For the catalyst with 30% functional group loading, its surface area and pore volume decreased to about 6% of that for the substrate material, therefore, the dispersion of the acid groups would lower drastically. The compromise between the increasing number of acid sites and the decreasing surface area and mesoscopic ordering led to an optimal functional group loading at 15% as exhibited in the transesterification reaction.

3.5. Surface hydrophobicity modification over Ar-SO_3H-10 catalyst

Due to the highly hydrophobic nature of both soybean oil and biodiesel product, their molecular transport within the pore framework is expected to be especially affected by surface interactions [26,38–40]. The Ar-SO_3H-10 catalyst was further functionalized with methyl silyl groups to modify its surface hydrophilicity–hydrophobicity balance with an attempt to improve its catalytic performance. Methyl groups were incorporated into the catalyst by capping with methoxytrimethyl silane using a post-synthetic method (C-Ar-SO_3H-10) and methylation with methyltriethoxy silane using a one-step synthetic method

Table 2
Textural and acid properties of Ar-SO_3H modified SBA-15 catalysts with variable function group loadings.

Sample	XRD		Textural properties			Acid properties[e]		
	d_{100}[a] (Å)	Wall thickness[b] (Å)	BET area (m^2/g)	Pore size[c] (Å)	Pore volume[d] (cm^3/g)	Sulfur (mequiv./g)	NaCl exchange (mequiv./g)	TMACl exchange (mequiv./g)
Ar-SO_3H-5	105	63.2	815	58	1.13	0.54	0.63	0.63
Ar-SO_3H-10	109	68.9	805	57	1.08	1.07	1.15	1.14
Ar-SO_3H-15	109	69.9	572	56	0.75	1.48	1.45	1.44
Ar-SO_3H-20	108	72.7	379	52	0.47	1.85	1.98	1.65
Ar-SO_3H-30	109	62.9	52	63	0.08	2.10	2.37	1.96

[a] d_{100} spacing measured from small-angle X-ray diffraction.
[b] Average pore wall thickness calculated by a_0-pore size ($a_0 = 2 \times d_{100}/\sqrt{3}$).
[c] Average pore size from adsorption branch applying the BJH model.
[d] Pore volume was taken at $P/P_0 = 0.985$ single point.
[e] Acid capacity defined as milliequivalents of acid centers per gram of catalyst, obtained either directly by titration or indirectly from the sulfur content by elemental analysis.

Table 3
Textural and acid properties of Ar-SO_3H-10 catalysts modified by capping with methoxytrimethyl silane and methylation with methyltriethoxy silane.

Sample	XRD		Textural properties			Acid properties[e]		
	d_{100}[a] (Å)	Wall thickness[b] (Å)	BET area (m^2/g)	Pore size[c] (Å)	Pore volume[d] (cm^3/g)	Sulfur (mequiv./g)	NaCl exchange (mequiv./g)	TMACl exchange (mequiv./g)
C-Ar-SO_3H-10	–	–	534	47	0.60	–	–	–
M-Ar-SO_3H-10	110	69.0	784	58	1.06	–	1.26	1.16

[a] d_{100} spacing measured from small-angle X-ray diffraction.
[b] Average pore wall thickness calculated by a_0-pore size ($a_0 = 2 \times d_{100}/\sqrt{3}$).
[c] Average pore size from adsorption branch applying the BJH model.
[d] Pore volume was taken at $P/P_0 = 0.985$ single point.
[e] Acid capacity defined as milliequivalents of acid centers per gram of catalyst, obtained either directly by titration or indirectly from the sulfur content by elemental analysis.

(M-Ar-SO_3H-10). The textural and acid properties of the modified catalysts are summarized in Table 3 and the XRD pattern of M-Ar-SO_3H-10 catalyst is shown in Fig. 8. The C-Ar-SO_3H-10 catalyst synthesized by a post-grafting method has a decreased surface area, pore size and pore volume which could be due to the pore blocking by methoxytrimethyl silyl groups, whereas the M-Ar-SO_3H-10 catalyst prepared by co-condensation has very similar properties as the unmodified Ar-SO_3H-10 catalyst, which is consistent with the similar observation for the catalysts synthesized by the above two methods previously. The small-angle XRD pattern in Fig. 8 confirmed that M-Ar-SO_3H-10 catalyst has similar hexagonally ordered mesoscopic structures and unit cell parameters (d_{100} and average pore wall thickness) to the unmodified Ar-SO_3H-10 catalyst.

These two modified catalysts were tested in the transesterification of soybean oil with 1-butanol at 190 °C, alcohol to oil molar ratio 6:1 and using 5 wt% of catalyst. The C-Ar-SO_3H-10 catalyst

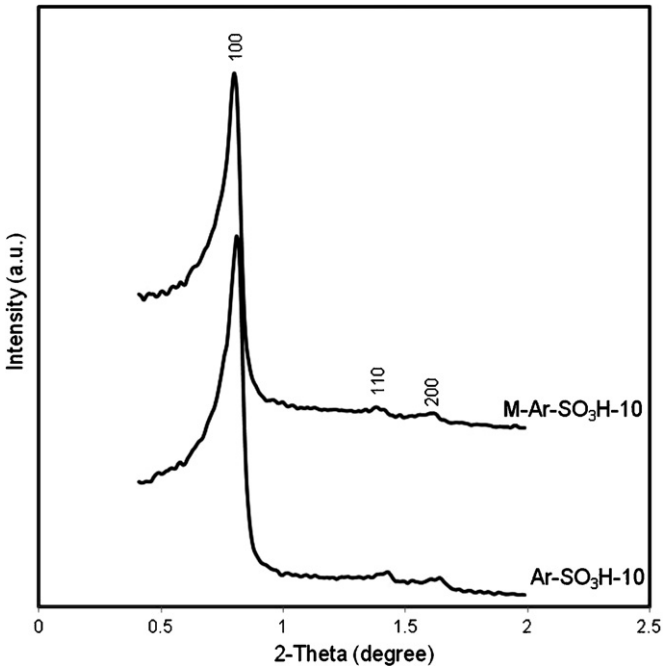

Fig. 8. Small-angle powder XRD pattern for methylated Ar-SO_3H-10 catalyst.

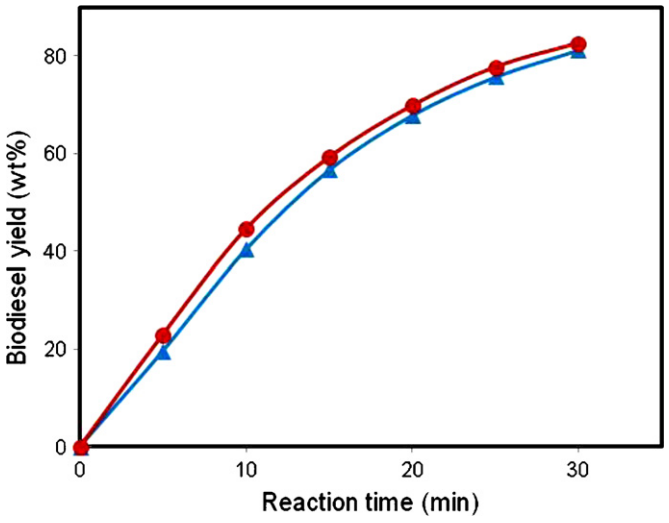

Fig. 9. Comparison of methylated Ar-SO_3H-10 catalyst (●) with unmodified Ar-SO_3H-10 catalyst (▲) in transesterification reaction. Reaction conditions: 3.0 g of soybean oil, 1.53 g of 1-butanol, 150 mg of catalyst, 190 °C, 30 min.

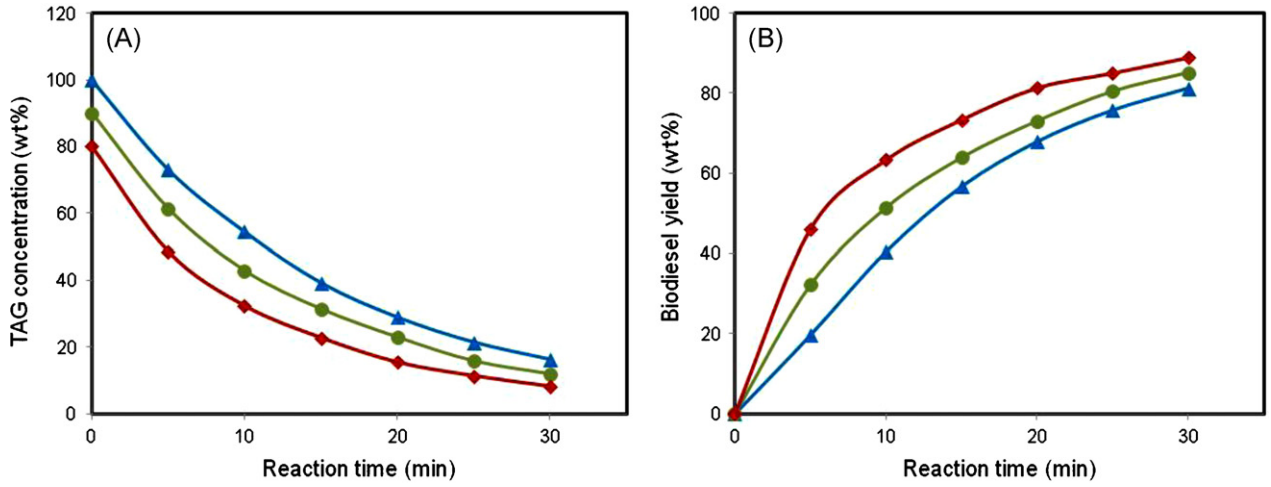

Fig. 10. Simultaneous esterification and transesterification reactions over Ar-SO_3H-10 catalyst. Reaction conditions: 3.0 g of soybean oil (▲) or 2.7 g of soybean oil + 0.3 g of oleic acid (●) or 2.4 g of soybean oil + 0.6 g of oleic acid (♦), 1.53 g of 1-butanol, 150 mg of catalyst, 190 °C, 30 min.

exhibited a lower activity than the unmodified Ar-SO_3H-10 catalyst (not shown). This may be due to the fact that some acid sites may have been blocked by the post-grafted methoxytrimethyl silyl groups as indicated by the decreased surface area and pore size in Table 3. The M-Ar-SO_3H-10 catalyst was only slightly more active than the unmodified Ar-SO_3H-10 catalyst as shown in Fig. 9 because of their similar textural and acid properties. Reuse of this catalyst after solvent washing gave a similar activity recovery (88%) as previously, indicating a similar behavior to that of Ar-SO_3H-10 catalyst in terms of reusability. The effect and mechanism of the incorporated hydrophobic groups on the catalyst performance will be further studied in future work.

3.6. Simultaneous esterification and transesterification

As mentioned in Section 1, it is desirable that solid acid catalysts can simultaneously catalyze the esterification and transesterification reactions when using low quality recycled oils or greases containing considerable amounts of free fatty acids as feedstock. For this purpose, the Ar-SO_3H-10 catalyst (one of the mesostructured acid catalysts showing good catalytic performance) was tested by using soybean oil mixed with 10 wt% and 20 wt% of oleic acid under the same reaction conditions used in the above screening of catalysts (reaction temperature of 190 °C, molar ratio of alcohol to oil 6:1 and 5 wt% catalyst weight). In both cases, the Ar-SO_3H-10 catalyst showed high activity and effectively catalyzed the esterification and transesterification reactions simultaneously. There was no unconverted oleic acid detected from the product samples collected at 5 min from both experiments indicating the esterification of oleic acid with 1-butanol is an easy and fast reaction under the present conditions. It can be seen from Fig. 10A that the presence of oleic acid slightly accelerated the conversion of triglycerides in soybean oil. The biodiesel yield presented in Fig. 10B apparently increased as the percentage of oleic acid in the feedstocks increased which again confirmed that the rate of esterification is faster than that of transesterification, in agreement with earlier reports [17,41]. The results demonstrate that the activity of this arene-sulfonic acid functionalized mesoporous catalyst was not affected by the presence of high amounts of free fatty acids up to 20 wt%, indicating that this catalyst could be a promising candidate for processing low quality feedstocks such as recycled waste oils or greases.

4. Conclusions

Propyl-SO_3H and arene-SO_3H functionalized SBA-15 catalysts have exhibited high activity and stability in the microwave-assisted transesterification of soybean oil with 1-butanol, whereas perfluoro-SO_3H functionalized SBA-15 catalyst yielded a complete loss of activity after recycling due to complete leaching of perfluoro-SO_3H groups in the reaction medium. Optimization results over arene-SO_3H functionalized catalyst have shown that the optimal loading of arene-SO_3H groups is around 15% (molar percent of functional group to total silicon), and the optimal oil to alcohol molar ratio is 1:6. The reaction rate increased more than proportionally to the increase in catalyst to oil weight ratio. Utilizing and recycling the catalyst at a high temperature of 240 °C demonstrated a significantly increased reaction rate and a good thermal stability. Further modification of Ar-SO_3H SBA-15 catalyst with hydrophobic groups did not significantly improve its catalytic performance. Combined transesterification and esterification of high FFA feedstocks over arene-SO_3H functionalized SBA-15 catalyst gave rise to increased reaction rates, indicating that this catalyst could be a promising candidate for processing low quality feedstocks containing high fraction of free fatty acids. In addition, the microwave-assisted reactor could provide a fast, easy reaction technology with advantages of a short reaction time and a low alcohol to oil molar ratio for biodiesel production.

Acknowledgements

This work was funded by the Army Research Laboratory, U.S. Department of Defense, under agreement W911NF-08-2-0029, and the University of Wisconsin System ARG Program.

References

[1] M. Diasakou, A. Louloudi, N. Papayannakos, Fuel 77 (1998) 1297–1302.
[2] J.M. Encinar, J.F. Gonzalez, E. Sabio, M.J. Ramiro, Industrial and Engineering Chemistry Research 38 (1999) 2927–2931.
[3] S.J. Clark, L. Wagner, M.D. Schrock, P.G. Piennaar, Journal of the American Oil Chemists Society 61 (1984) 1632–1638.
[4] C.L. Peterson, D.L. Reece, B.J. Hammond, J. Thompson, S.M. Beck, ASAE Paper 9 (1994) 4–6531.
[5] F. Ma, M.A. Hanna, Bioresource Technology 70 (1999) 1–15.
[6] M. Bender, Bioresource Technology 70 (1999) 81.
[7] F. Ma, L.D. Clements, M.A. Hanna, Industrial and Engineering Chemistry Research 37 (1998) 3768.
[8] M. Canakci, J. Van Gerpen, ASAE Transactions 46 (2003) 945–954.
[9] M. Di Serio, R. Tesser, P. Lu, E. Santacesaria, Energy & Fuels 22 (2008) 207–217.

[10] M. Canakci, J. Van Gerpen, Transactions of the American Society of Agricultural Engineers 44 (2001) 1429–1436.
[11] G.W. Huber, S. Iborra, A. Corma, Chemical Reviews 106 (2006) 4044–4098.
[12] M.G. Kulkarni, A.K. Dalai, Industrial and Engineering Chemistry Research 45 (2006) 2901–2913.
[13] E. Lotero, J.G. Goodwin Jr., D.A. Bruce, K. Suwannakarn, Y. Liu, D.E. Lopez, Catalysis 19 (2006) 41–84.
[14] R. Tesser, M. Di Serio, M. Guida, M. Nastasi, E. Santacesaria, Industrial and Engineering Chemistry Research 22 (2005) 7978–7982.
[15] S. Pasias, N. Barakos, C. Alexopoulos, N. Papayannakos, Chemical Engineering and Technology 29 (2006) 1365–1371.
[16] D.E. López, J.G. Goodwin Jr., D.A. Bruce, E. Lotero, Applied Catalysis A-General 295 (2005) 97–105.
[17] M.G. Kulkarni, R. Gopinath, L.C. Meher, A.K. Dalai, Green Chemistry 8 (2006) 1056–1062.
[18] F. Chai, F. Cao, F. Zhai, Y. Chen, X. Wang, Z. Su, Advanced Synthesis and Catalysis 349 (2007) 1057–1065.
[19] A. Baig, F.T.T. Ng, Energy and Fuels 24 (2010) 4712–4720.
[20] D.E. López, J.G. Goodwin Jr., D.A. Bruce, S. Furuta, Applied Catalysis A-General 339 (2008) 76–83.
[21] Y.-M. Park, D.-W. Lee, D.-K. Kim, J.-S. Lee, K.-Y. Lee, Catalysis Today 131 (2008) 238–243.
[22] C.M. García, S. Teixeira, L.L. Marciniuk, U. Schuchardt, Bioresource Technology 99 (2008) 6608–6613.
[23] S. Furuta, H. Matsuhashi, K. Arata, Catalysis Communications 5 (2004) 721–723.
[24] S. Furuta, H. Matsuhashi, K. Arata, Biomass and Bioenergy 30 (2006) 870–873.
[25] I.K. Mbaraka, D.R. Radu, V.S.-Y. Lin, B.H. Shanks, Journal of Catalysis 219 (2003) 329–336.
[26] J.A. Melero, L.F. Bautista, G. Morales, J. Iglesias, R. Sanchez-Vazquez, Chemical Engineering Journal 161 (2010) 323–331.
[27] J.A. Melero, R. van Grieken, G. Morales, Chemical Reviews 106 (2006) 3790–3812.
[28] N.E. Leadbeater, L.M. Stencel, Energy & Fuels 20 (2006) 2281–2283.
[29] T.M. Barnard, M.B. Boucher, N.E. Leadbeater, L.M. Stencel, B.A. Wilhite, Energy & Fuels 21 (2007) 1777–1781.
[30] J. Geuens, J.M. Kremsner, B.A. Nebel, S. Schober, R.A. Dommisse, M. Mittelbach, S. Tavernier, C.O. Kappe, B.U.W. Maes, Energy & Fuels 22 (2008) 643–645.
[31] G. Knothe, Fuel Processing Technology 86 (2005) 1059–1070.
[32] I. Lee, L.A. Johnson, E.G. Hammond, Journal of the American Oil Chemists Society 72 (1995) 1155–1160.
[33] R.O. Dunn, M.W. Shockley, M.O. Bagby, Journal of the American Oil Chemists Society 73 (1996) 1719–1728.
[34] D. Margolese, J.A. Melero, S.C. Christiansen, B.F. Chmelka, G.D. Stucky, Chemistry of Materials 12 (2000) 2448–2459.
[35] J.A. Melero, G.D. Stucky, R. van Grieken, G. Morales, Journal of Materials Chemistry 12 (2002) 1664–1670.
[36] S. Miao, B.H. Shanks, Applied Catalysis A-General 359 (2009) 113–120.
[37] D. Zhao, J. Feng, Q. Huo, N. Melosh, G.H. Fredrickson, B.F. Chmelka, G.D. Stucky, Science 279 (1998) 548–552.
[38] I. Díaz, C. Márquez-Alvárez, F. Mohino, J. Pérez-Pariente, E. Sastre, Journal of Catalysis 193 (2000) 295–302.
[39] Q. Yang, M.P. Kapoor, N. Shirokura, M. Ohashi, S. Inagaki, J.N. Kondo, K.J. Domen, Journal of Materials Chemistry 15 (2005) 666–673.
[40] B. Show, S. Hamoudi, M.H. Zahedi-Niaki, S. Kaliaguine, Microporous and Mesoporous Materials 79 (2005) 129–136.
[41] Y. Warabi, D. Kusdiana, S. Saka, Bioresource Technology 91 (2004) 283–287.